Relay Node Selection and Power Allocation for Distributed Self-Concatenated Convolutional Codes

Haji Muhammad Furqan Ahmed Madni[1,2], Muhammad Fasih Uddin Butt[1], Nida Zamir[1] and Soon Xin Ng[3]

[1]Department of Electrical Engineering, COMSATS Institute of Information Technology (CIIT), Islamabad 44000, Pakistan (Email: fasih@comsats.edu.pk).

[2]School of Engineering and Natural Sciences, Istanbul Medipol University, Istanbul, Turkey (Email: hamadni@st.medipol.edu.tr).

[3]School of Electronics and Computer Science, University of Southampton, SO17 1BJ, Southampton, U.K. (Email: sxn@ecs.soton.ac.uk).

***Abstract*— In this contribution, the performance of a Distributed Self-Concatenated Convolutional Coding (DSECCC) scheme is analyzed by using Iterative Decoding (ID) for cooperative communications (CC) with the aid of relay selection (RS) and power allocation (PA). In the RS based DSECCC-ID scheme, where the transmit Signal to Noise power Ratio (SNR) is equal for both source and relay, we can achieve the minimum value of the required SNR at both destination and relay simultaneously by choosing a relay at an appropriate geographical location. By contrast, in the PA based DSECCC-ID scheme, where the position of the relay is in the middle, minimum required transmit SNRs are used both at the source and the relay. These schemes are analyzed with the help of binary Extrinsic Information Transfer (EXIT) charts. From our simulation results, we found that the RS based DSECCC-ID scheme outperforms the PA based DSECCC-ID scheme.**

I. Introduction

Future wireless communication systems must support excessively high data rates for wireless internet and other multimedia services at a given limited bandwidth and power. Therefore, the demand for bandwidth efficient transceivers is increasing day by day [1]. In order to support higher data rates, Multiple-Input Multiple-Output (MIMO) techniques can be utilized [2]. However, for a pocket sized mobile device, there is limited antenna spacing, which results in signal's correlation. So, MIMO system cannot be implemented efficiently in such small sized systems [3]. CC [4] can be used as an alternative to MIMO for pocket sized mobiles, since it not only eliminates the correlation but also achieves MIMO like diversity gain. CC is defined as a type of communication system that allows the source to route data towards destination through a relay placed between the destination and the source [5]. The most common CC types are Amplify-and-Forward (AF) and Decode-and-Forward (DF). In order to avoid enhancement of noise in AF scheme and to mitigate the propagation of error in the DF scheme, an effective channel code is required [5], [6]. Distributed Coding (DC) [7] is a special type of coding in which there is a joint design of coding between source and relay. With the help of iterative detection at relay and destination, DC schemes can approach the achievable capacity of the relay channel. Many DC schemes have been proposed for CC in literature, such as, Distributed Turbo Trellis Coded Modulation [8], Distributed Low Density Parity Check Codes [9, 10], Distributed Turbo Codes [11–14], Distributed Space-Time Codes [15–18], Distributed Self-Concatenated Convolutional Codes using Iterative Decoding (DSECCC-ID) [19], Distributed Rateless Codes [20] and Distributed Soft Coding [21].

In addition to that, relay node selection based on high quality links between source to relay and relay to destination have been shown to enhance the efficiency of power in relay network [22], [23]. EXIT chart [24] analysis is one of the best tools to analyze iterative decoding schemes and to predict the minimum required receive SNR for very low value of BER without consuming time in performing bit-by-bit decoding. DSECCC-ID scheme for half duplex relay aided cooperative communications using EXIT chart analysis was investigated in [19].

In this contribution, the DSECCC-ID scheme that was presented in [19] is extended by applying relay node selection (RS) and power allocation (PA) mechanism [22], [25–27]. We found that:

1) *The realistic case of RS-DSECCC-ID scheme is* 0.72 *dB better, while the PA-DSECCC-ID scheme is* 0.11 *dB better than the DSECCC-ID scheme of [19].*
2) *The RS-DSECCC-ID scheme is* 1.28 *dB away, while the PA-DSECCC-ID scheme is* 1.4 *dB away from their respective channel capacity related SNR limits.*

Hence, the proposed RS-DSECCC-ID schemes and PA-DSECCC-ID schemes outperform the DSECCC-ID scheme of [19] and operate closer to their channel capacity related SNR limits.

The rest of the paper is organized in the following way: The system model is presented in Section II, while Section III describes the RS-DSECCC-ID and PA-DSECCC-ID schemes as well as their corresponding EXIT charts and relay channel capacity investigations. In Section IV, simulation results are presented and paper is concluded in Section V.

II. System Model

Our system model consists of a source (S), a relay (R) and a destination (D) nodes, as presented in Fig. 1. It is a two-hop half duplex DF CC system, employing Time Division Multiple Access (TDMA) protocol. S transmits the frame of encoded symbols $\{x_s\}$ to R and D during the transmission period T_1. R first decodes the received symbols and then passes them to the encoder. After re-encoding, R forwards the encoded symbols $\{x_r\}$ to D during the transmission period, T_2. Our system suffers from the free-space path loss and

978-1-5090-4183-1/17/$31.00 ©2017 IEEE

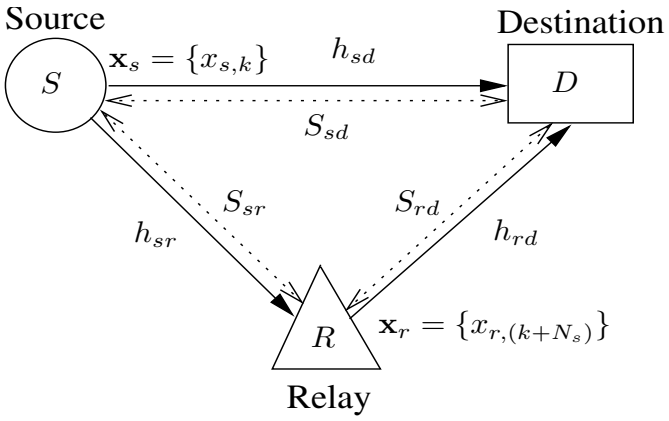

Fig. 1. System Model of our CC system [19].

the uncorrelated Rayleigh fading effects [4]. In Fig. 1, the notations S_{sd}, S_{sr} and S_{rd} denote the S-D, S-R and R-D distances, respectively. Similarly, the notations h_{ab}, n_{ab} and $P(ab)$ denote the Rayleigh fading coefficient, the zero-mean complex additive white Gaussian noise (AWGN) with variance of $N_0/2$ per dimension and the free space path loss between the node pair (a, b), respectively. $P(ab)$ is given by

$$P(ab) = K/S_{ab}^{\alpha}, \tag{1}$$

where $\alpha = 2$ is the free space path loss exponent, K is an environment dependent constant and S_{ab} represents the distance between a and b node. The relationship between the energy received at D (E_{sd}) and the energy received at R (E_{sr}), is given by [27] as

$$E_{sr} = \frac{P(sr)}{P(sd)} E_{sd} = G_{sr} E_{sd}. \tag{2}$$

Here, $G_{sr} = \left(\frac{S_{sd}}{S_{sr}}\right)^2$ represents the path gain for S-R link with respect to S-D link due to Reduced Distance. At R, the kth received signal during the 1st transmission period T_1, is given by:

$$y_{sr,k}^{(T1)} = \sqrt{G_{sr}} h_{sr,k}^{(T1)} x_{sr,k}^{(T1)} + n_{sr,k}^{(T1)}, \tag{3}$$

In comparison, at D, the kth received symbol during T_1, is given by:

$$y_{sd,k}^{(T1)} = h_{sd,k}^{(T1)} x_{sd,k}^{(T1)} + n_{sd,k}^{(T1)}, \tag{4}$$

Similarly, at D, the lth symbol received in the 2nd period of transmission T_2, is given by:

$$y_{rd,l}^{(T2)} = \sqrt{G_{rd}} h_{rd,l}^{(T2)} x_{rd,l}^{(T2)} + n_{rd,l}^{(T2)}, \tag{5}$$

where $l \in \{1 + N_s, ..., N_r + N_s\}$. The path-gain for the R-D link relative to the S-D link is $G_{rd} = \left(\frac{S_{sd}}{S_{rd}}\right)^2$.

A. Channel Encoder

In this work, an SECCC encoder is employed at S and a Recursive Systematic Convolutional (RSC) encoder is employed at R [19], both assisted by Quadrature Phase-Shift Keying (QPSK) modulation. R detects and decodes the received signal using SECCC decoder during T_1. The decoded bits at R are first interleaved by random bit interleaver π_r before encoding by RSC encoder during T_2. It should be noted that only parity bits of the RSC encoder are transmitted to D [19]. As shown in Fig. 2, the encoders used at both S and R can be considered as a 3-component parallel concatenated SECCC encoder, where a decoder having two decoding iterations can be invoked for detecting the information bits. At the source node, a rate-1/3 SECCC encoder employing QPSK modulation is considered. It is operating close to the S-R link capacity. The input bit stream $\{b_1\}$ of SECCC encoder is passed through an interleaver, which yields a stream $\{b_2\}$. These streams are then passed through parallel-to-serial converter and the resultant bit stream is sent to the RSC encoder (having a rate $R_1 = 1/2$). After that, the bit stream is fed to the interleaver and then to a puncturer (having a rate $R_2 = 3/4$). So, overall code rate R becomes 1/3, where $R = R_1/(2 \times R_2)$. The resultant bit stream is then mapped to 2-bit QPSK symbols using bit-to-symbol mapping function $\mu(.)$. The 2-bit QPSK symbol is represented by $x = \mu(c_1 c_0)$. These symbols are then transmitted over the channel. The bandwidth efficiency for this system is given by $\eta_1 = R \times \log_2(4)$ = 0.67 bit/s/Hz. In Fig. 2, x_r denotes a QPSK symbol at R, while puncturer is represented by R_4. In this scheme, it is sufficient to transmit parity bits from R, so that, all of the information bits are punctured in order to improve the overall throughput. The overall throughput for this case can be shown as

$$\eta = \frac{N_i}{N_s + N_r}, \tag{6}$$

where, N_r is number of modulated symbols per frame transmitted by R, N_s is number of modulated symbols per frame transmitted by S and N_i is the number of information bits which are being transmitted during the symbol periods $(N_s + N_r)$. For this case, N_s = 180,000 symbols, N_i = 120,000 bits and N_r = 60,000. So that, the overall value of the effective throughput of DSECCC-ID scheme is η =0.5 BPS. The relationship of E_b/N_0 versus SNR per bit is given by E_b/N_0 = SNR/η. It should be noted that the conventional SECCC scheme, is 1.25 dB better than DSECCC-ID in term of E_b/N_0.

B. Channel Decoder

The block diagram of DSECCC-ID decoder is presented in Fig. 2. The notations $L(.)$ and $P(.)$ are Logarithmic-Likelihood Ratio (LLR) of bit probabilities and the logarithmic-domain symbol probabilities, respectively. The unique nature of probabilities and LLRs are represented by subscripts o, e and a denoting $aposteriori$, $extrinsic$ and $apriori$ information, respectively, while, notations (c) and (b) represent coded bits and information bits, respectively. The DSECCC decoder consists of two components, namely the SECCC decoder and the RSC decoder. The SECCC decoder denoted as component (1) can also be considered as a two component decoder employing $I_{sd} = 4$ self-concatenated iterations. The received signal first passed through the soft demapper of SECCC decoder, where the conditional probability density function (CPDF) of receiving $y_1^T(d)$ is calculated, when x_s^m was transmitted, where $x_s^m = \mu(c_1, c_0)$ is the transmitted QPSK symbol for $s \in (0, 1, 2, 3)$. The signal that

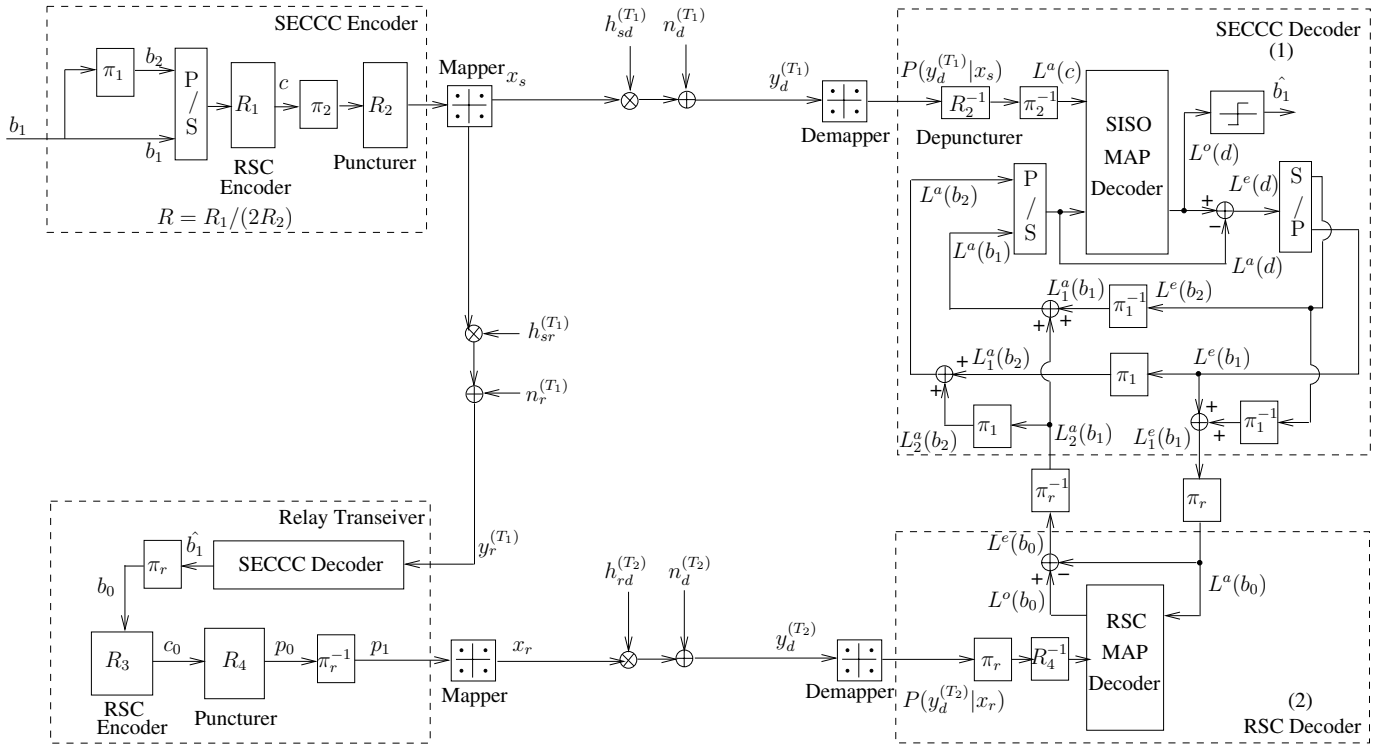

Fig. 2. The schematic of the DSECCC-ID Encoder and Decoder.

is received at soft demapper of the RSC decoder (denoted as component (2)) is used to find out CPDF of receiving $y_2^T(d)$, when x_r^m was transmitted. These bit probabilities are then fed to a soft depuncturer. The soft depuncturer converts these probabilities to the respective LLRs and afterwards inserts zero LLRs at the punctured bit positions. The LLRs are then passed through deinterleaver and then fed to the Soft-Input Soft-Output (SISO) RSC Maximum A Posteriori Probability (MAP) decoder. RSC MAP decoder block is fed with $L^a(b_0)$, which is the interleaved version of $L_1^e(b_1)$ that is calculated by summing up $L^e(b_1)$ and $L^e(b_2)$, as shown in Fig. 2. The second input to the RSC MAP decoder block is formed by interleaving and depuncturing of $P(y_d^{T_2}|x_r)$, which is the soft information that is provided by the QPSK demapper. The RSC decoder then generates $L^e(b_0)$ as its output. The LLR $L^e(b_0)$ is deinterleaved by π_r^{-1} to obtain $L_2^a(b_1)$. The resultant output can be further interleaved by using π_1 to generate $L_2^a(b_2)$. These *apriori* LLRs are then added to the SECCC decoder's *apriori* LLRs of b_1 and b_2, hence the iteration between the RSC and the SECCC decoder is complete.

III. Power Allocation and Relay Node Selection based DSECCC-ID

In this contribution, DSECCC-ID scheme is extended with the help of PA and RS. We design a system, which simultaneously achieves minimum required receive SNR at R and D nodes such that a BER value lower than 10^{-5} is achieved, thus ensuring minimum error propagation. In DSECCC-ID scheme the relay is considered to be placed in the middle of source and destination nodes and equal transmit SNR (SNR_t^s) is used at both source and relay nodes, whose value is much more than the minimum required receive SNR value [27] given as

$$SNR_r^{sr} = SNR_t^s + 10\log_{10}(G_{sr})[dB] \tag{7}$$

As compared to simple DSECCC-ID, in PA-DSECCC-ID scheme, only minimum required transmit SNR values are used at S and R nodes, while inn RS-DSECCC-ID scheme equal transmit SNR is used at S and R nodes that is less than the minimum required SNR. In RS case, the minimum required receive SNR value is calculated by selecting R at an appropriate geographical location.

A. Power allocation based DSECCC-ID

PA-DSECCC-ID is used to improve power efficiency in those situations when R nodes are limited in number and have fixed locations [25–27]. Here, it is assumed that R is placed in the middle of both S and D nodes. The design of PA-DSECCCC-ID is performed using three step EXIT charts procedure. The first step involves finding the decoding convergence of SECCC scheme that is employed at the $S-R$ link having code memory $v = 3$, as presented in Fig. 21 of [19], which gives the minimum required receive SNR at R as $SNR_r^{sr} = -0.15$. In the second step, the decoding convergence at D is analyzed. Finally in the last step, decoding trajectory is computed to verify the EXIT chart analysis. It should be noted that the tunnel remains closed at a lower SNR than this value. We can achieve the receive SNR value of -0.15 dB by selecting various combinations of SNR_t^s and G_{sr}. Since R has been placed in the middle of both S and D nodes, so $G_{sr} = G_{rd} = 4$. Hence, $SNR_t^s = -0.15 - 6.02 = -6.17$ dB, while the receive SNR at D from R is represented by

$$SNR_r^{rd} = SNR_t^r + 10\log_{10}(G_{rd})[dB], \tag{8}$$

where, SNR_t^r is the transmit SNR from R. In the following discussion the decoding convergence of PA-DSECCC-ID scheme is analyzed by using EXIT chart. The EXIT curves of the SECCC decoder and RSC decoder for S-D link and R-D link, respectively, are recorded and plotted, as shown in Fig. 3. The EXIT curves associated with the SECCC decoder and the RSC decoder do not intersect when we have $SNR_t^s = -6.17$ dB and $SNR_t^{rd} = 0.22$ dB, respectively. Code memories $v = 2$ and $v = 3$ are used by the RSC encoder at R and by the SECCC encoder at S, respectively. In the next step, the

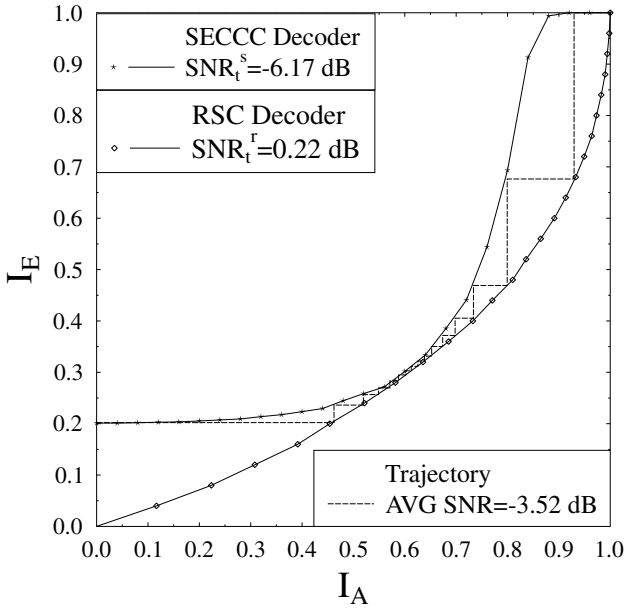

Fig. 3. EXIT chart analysis of PA-DSECCC-ID scheme.

decoding trajectory is computed using Monte Carlo simulation for the PA-DSECCC-ID scheme to verify the analysis of EXIT charts. The decoding trajectory based on a frame length of 120000 bits when $SNR_t^s = -6.17$ dB and $SNR_t^r = 0.22$ dB, is depicted in Fig. 3. A good match verifies that the prediction by EXIT charts is accurate. It should be noted from Fig. 3 that the minimum receive SNR needed during T_1 at R is given by $SNR_r^{sr} = -0.15$ dB, while the minimum receive SNR required during T_2 at D is given by $SNR_r^{rd} = 6.24$ dB. In order to achieve $SNR_r^{sr} = -0.15$ dB at R, the corresponding transmit SNR at S is given by $SNR_t^s = -6.17$ dB. Since, we have $G_{sd} = 1$, the value of receive SNR at D during T_1 is given by $SNR_r^{sd} = SNR_t^s = -6.17$ dB. The receive SNR needed during T_2 at D is given by $SNR_r^{rd} = 6.24$ dB and the transmit SNR at R is given by $SNR_t^r = 0.22$ dB. The average value of the transmit SNR of our PA based scheme can be calculated as

$$SNR = 10 \times \log(\lambda 10^{\frac{SNR_t^s}{10}} + (1-\lambda)10^{\frac{SNR_t^r}{10}}), \qquad (9)$$

where the value of SNR is equal to -3.52 dB for $SNR_t^r = 0.22$ dB and $SNR_t^s = -6.17$ dB and $\lambda = 3/4$ [19].

B. Relay Node Selection based DSECCC-ID

From the earlier section, it is clear that the minimum required receive SNR value at S is 6.24, while at R is -0.15.

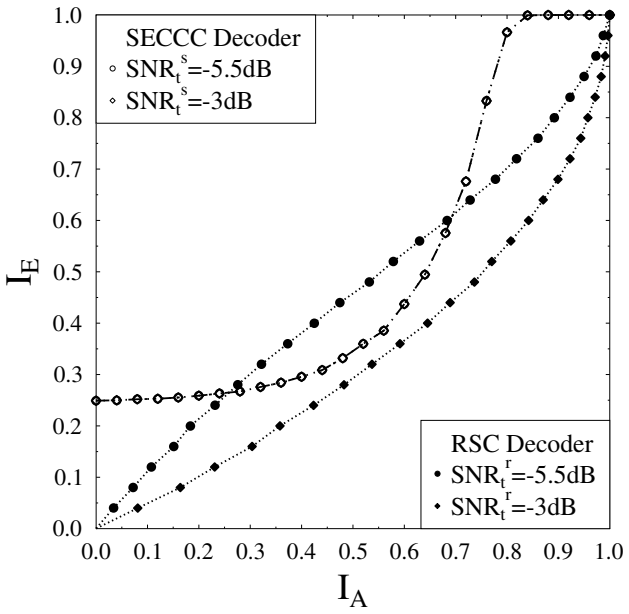

Fig. 4. EXIT chart analysis of RS-DSECCC-ID scheme for non-optimal SNR values.

In this scheme, instead of using the minimum required receive SNR at both S and R, the value of transmit SNR is fixed to a constant value of f (i.e $f = SNR_t^s = SNR_t^r$) at both of these nodes. The minimum required SNR is then attained simultaneously at the nodes by selecting R (located in direct $S-R$ path) at an appropriate geographical location and achieving different values of G_{sr} and G_{rd} [25–27]. The value of G_{sr} can be calculated from the following formula [27]:

$$G_{sr} = 10^{\frac{SNR_r^{sr} - SNR_t^s}{10}}, \qquad (10)$$

while G_{rd} can be calculated by [27]:

$$G_{rd} = \frac{1}{1 - \frac{1}{\sqrt{G_{sr}}}}, \qquad (11)$$

The design procedure using EXIT charts consists of finding the optimal value of SNR for which the tunnel is open and then finding the corresponding R position. The EXIT curves for the same value of SNR_t at S and R are plotted in Fig. 4 and is repeated for a range of SNR values but we present only few values for simplicity. It should be noted from Fig. 4 that the EXIT curves and the tunnel remain closed at lower values of SNR, for example, at -5.5 dB. The tunnel remains wide open at higher values of SNR, for example -3 dB. At -5.5 dB, the corresponding path gains are $G_{sr} = 3.42$ and $G_{rd} = 4.72$ corresponding to $d_{sr} = 0.54$ and $d_{rd} = 0.45$, respectively. By contrast, at -3 dB, the path gains are $G_{sr} = 1.93$ and $G_{rd} = 12.7$ which correspond to $d_{sr} = 0.72$ and $d_{rd} = 0.27$, respectively. This means that when the position of R is closer to D, the performance is better as compared to case when it is moved towards S.

The optimal SNR value at which the tunnel is just open is -4.5 dB, as presented in Fig. 5. The corresponding path gains are $G_{sr} = 2.72$ and $G_{rd} = 6.44$, which gives $d_{sr} = 0.61$ and

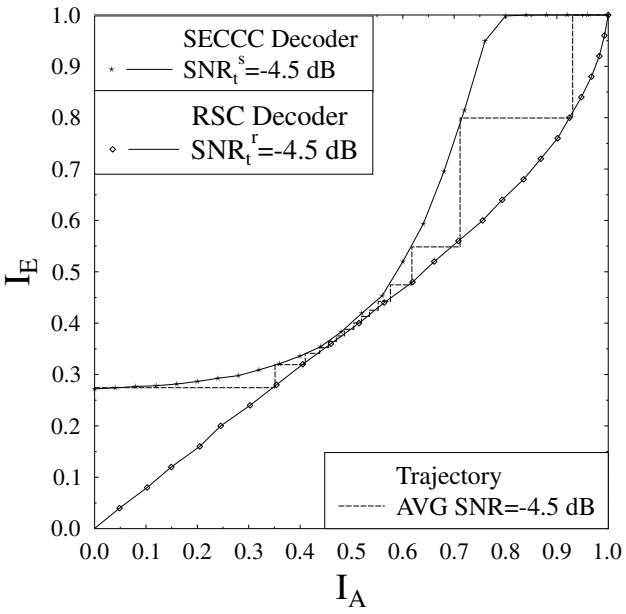

Fig. 5. EXIT chart analysis of RS-DSECCC-ID scheme for an optimal SNR value.

$d_{rd} = 0.39$, respectively. The average value of transmit SNR for the optimal case is given as

$$SNR = SNR_t^s = SNR_t^r = SNR_r^{sr} - 10\log(G_{sr}), \quad (12)$$

where, we have $SNR = -4.5$ dB for this case.

C. Capacity Curves

The capacity of a two-hop half-duplex relay channel has been calculated by employing the modified capacity equation derived in [28]. We consider the capacity of channels between S, R and D nodes to calculate the upper C^U and the lower bound limit C^L as follows [18, 19]:

$$C^U = \min\left\{\lambda C_{(s\to r,d)}, \lambda C_{(s\to d)} + (1-\lambda)C_{(r\to d)}\right\} \quad (13)$$

$$C^L = \min\left\{\lambda C_{(s\to r)}, \lambda C_{(s\to d)} + (1-\lambda)C_{(r\to d)}\right\} \quad (14)$$

where, $C_{(a\to b)}$ and $C_{(a\to b,c)}$ represents capacity of channel between the transmitter at node a and the receiver at node b and receivers at nodes (b and c), respectively. Here, we only consider the modulation dependent Discrete-input Continous-output Memoryless Channel (DCMC) capacity [29]. Capacity curves for RS, PA and non-cooperative case are presented in Fig. 6. The path gain values are $G_{sr} = 4$ and $G_{rd} = 4$ for the PA-DSECCC-ID scheme, while $G_{sr} = 2.72$ and $G_{rd} = 6.44$ are for the RS-DSECCC-ID case. Here SNR is the average transmit SNR.

The lower and upper bound capacity curves for relay's channel are presented in Fig. 6 for $\lambda = \frac{3}{4}$. It should be noted that these curves are based on the $4PSK$ DCMC. This scheme, as depicted in Fig. 6, has an SNR limit of 1.84 dB for the direct link (non-cooperative) and achieves a throughput of 1 Bit Per Symbol (BPS). The upper and lower bounds of the relay channel capacity for RS-DSECCC-ID have an SNR limit of approximately -5 dB for a throughput of 0.5 BPS, while those of the PA-DSECCC-ID have an SNR limit of approximately -5.5 dB for a throughput of 0.5 BPS. The upper bound equals the lower bound for both RS-DSECCC-ID and PA-DSECCC-ID at a throughput of 0.5 BPS. The SNR limit for RS-DSECCC-ID scheme outperforms the PA-DSECCC-ID scheme by 1 dB. It should be noted that the relay channel capacity bounds (both C^U and C^L) are higher than that of the direct link for a throughput under 1.2 BPS. This is because of the reduced path loss introduced by R. However, the asymptotic capacity of the direct link for throughput value above 1.2 BPS is higher than that of the relay channel due to the half-duplex constraint.

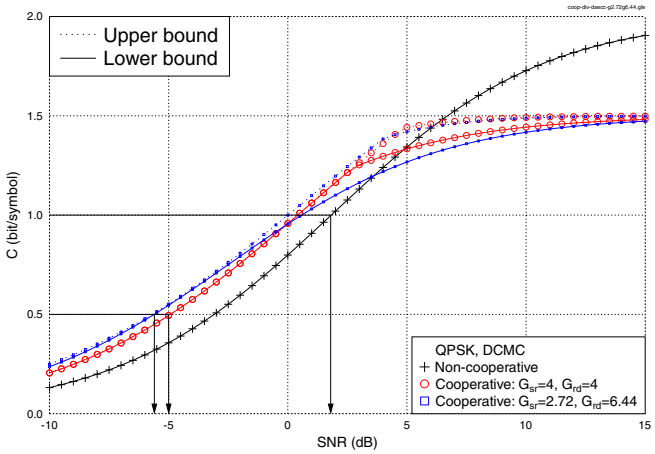

Fig. 6. The relay channel's upper and lower bound DCMC capacity curves.

We also found from the lower bound curves that the PA-DSECCC-ID scheme would enjoy a lower SNR limit than the RS-DSECCC-ID scheme when a higher rate SECCC is used, where a throughput of higher than 0.9 BPS is attained.

IV. Results and Discussions

This section investigates the BER versus average transmit SNR performance of DSECCC-ID, as shown in Fig. 7, when PA and RS are employed. The BER results have been plotted for both perfect and realistic S-R links. In realistic case, decoding errors may occur at R. The SNR threshold for perfect case of the DSECCC-ID scheme is -3.6 dB, while for RS, it is -4.34 dB and that for PA scheme is -3.72 dB. The threshold value at which a 'waterfall-like' shape of the BER curve occurs may be predicted by using EXIT chart, as presented in Section III. SNR threshold value for realistic case of the DSECCC-ID scheme is -3.5 dB, for the RS-DSECCC-ID is -4.22 dB and for the PA-DSECCC-ID scheme is -3.61 dB. The realistic RS-DSECCC-ID scheme is 3.3 dB better than simple SECCC-ID (non-cooperative) scheme at a BER of 10^{-5} [19]. Furthermore, the RS-DSECCC-ID scheme using realistic relay link assumption is 0.72 dB better than DSECCC-ID scheme at a BER of 10^{-5}. By contrast, PA-DSECCC-ID scheme is 0.11 dB better than the DSECCC-ID scheme. The difference between convergence thresholds for realistic and perfect curve for RS-SECCC-ID scheme is 0.12, while the difference is 0.11 for PA-DSECCC-ID scheme. RS-DSECCC-ID scheme has a capability to perform within about 1.28 dB from the relay-aided DCMC capacity of -5.5 dB at 0.5 BPS, where

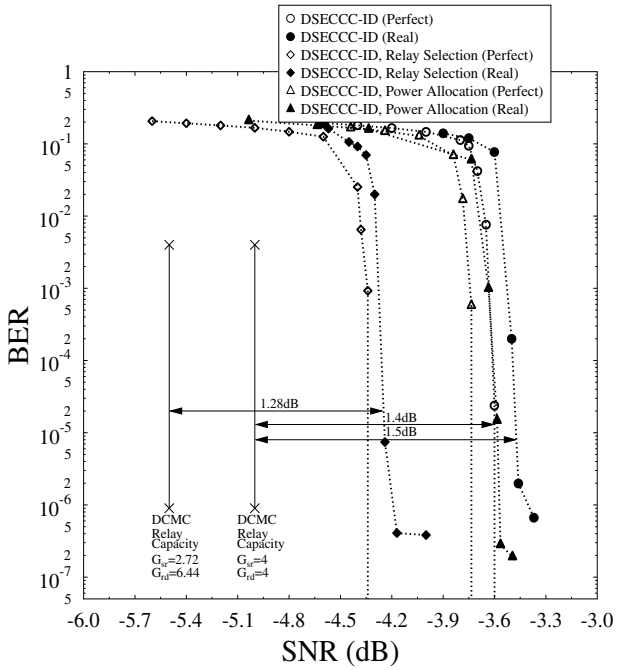

Fig. 7. BER curves for DSECCC-ID, PA-DSECCC-ID and RS-DSECCC-ID schemes.

$G_{sr} = 2.72$ and $G_{rd} = 6.44$. Furthermore, PA-DSECCC-ID scheme is 1.4 dB away from its relay-aided DCMC capacity of -5 dB at 0.5 BPS, where $G_{sr} = 4$ and $G_{rd} = 4$. Finally, the DSECCC-ID scheme is 1.5 dB away from its relay-aided DCMC capacity of -5 dB at 0.5 BPS, where $G_{sr} = 4$ and $G_{rd} = 4$, as shown in Fig. 7.

V. Conclusions and Future work

In this work, we have applied PA and RS mechanisms to the DSECCC-ID scheme of [19]. The perfect as well as realistic relay node based cooperative scenarios is considered. It has been shown that RS-DSECCC-ID scheme is 0.72 dB better, while PA-DSECCC-ID scheme is 0.11 dB better in performance than that of the DSECCC-ID scheme at a BER of 10^{-5}. The RS-DSECCC-ID scheme is 1.28 dB away from its capacity, which is 0.5 BPS at -5.5 dB, while PA-DSECCC-ID scheme is 1.4 dB away from its capacity, which is 0.5 BPS at -5 dB. Our simulation results agree with the relay channel capacity analysis. As seen from Fig. 7, all the three DSECCC-ID schemes employing realistic relay node perform closely to their perfect relay node based schemes. Finally, we have demonstrated that both PA and RS mechanisms further enhance the DSECCC-ID scheme.

References

[1] L. Hanzo, L. L. Yang, E. L. Kuan and K. Yen, *Single-and multi-carrier DS-CDMA: multi-user detection, space-time spreading, synchronisation, standards and networking*. John Wiley & Sons, 2003.

[2] L. Hanzo, S. X. Ng, T. Keller and W. Webb, *Quadrature amplitude modulation: From basics to adaptive trellis-coded, turbo-equalised and space-time coded OFDM, CDMA and MC-CDMA systems*. John Wiley & Sons, 2nd ed., 2004.

[3] L. Hanzo, O. Alamri, M. El-Hajjar and N. Wu, *Near-capacity multi-functional MIMO systems*. John Wiley and sons Ltd and IEEE Press, April 2009.

[4] K. J. K. Liu, A. K. Sadek, W. Su and A. Kwasinski, *Cooperative communications and networking*. Cambridge University Press, 2009.

[5] X. Tao, X. Xu and Q. Cui, "An overview of cooperative communications," *IEEE Communications Magazine*, vol. 50, pp. 65–71, 2012.

[6] M. Janani, A. Hedayat, T. Hunter and A. Nosratinia, "Coded cooperation in wireless communications: space-time transmission and iterative decoding," *IEEE Transactions on Signal Process*, vol. 52, pp. 362–371, 2004.

[7] Y. Li, "Distributed coding for cooperative wireless networks: An overview and recent advances," *IEEE Communications Magazine*, vol. 47, pp. 71–77, 2009.

[8] S. X. Ng, Y. Li and L. Hanzo, "Distributed turbo trellis coded modulation for cooperative communications ," in *International Conference on Communications (ICC)*, (Dresden, Germany), 2009.

[9] A. Chakrabarti, A. Baynast, A. Sabharwal and B. Aazhang, "Low density parity check codes for the relay channel," *IEEE Transactions on Wireless Communications*, vol. 6, pp. 3384–3394, 2007.

[10] P. Razaghi and W. Yu, " Bilayer low-density parity-check codes for decode-and-forward in relay channels," *IEEE Transactions on Wireless Communications Transactions on Information Theory*, vol. 53, pp. 3723–3739, 2007.

[11] B. Zhao and M. C. Valenti, "Distributed turbo coded diversity for relay channel," *IEEE Electronics Letters*, vol. 39, pp. 786–787, 2003.

[12] M. Janani, A. Hedayat and A. Nosratinia, "Coded cooperation in wireless communications: space-time transmission and iterative decoding ," *IEEE Transactions on Signal Processing*, vol. 52, pp. 326–371, 2004.

[13] Z. Zhang and T. Duman, "Capacity-approaching turbo coding for half-duplex relaying," *IEEE Transactions on Communications*, vol. 55, pp. 1895–1906, 2007.

[14] Y. Li, B. Vucetic and J. Yuan, "Distributed turbo coding with hybrid relaying protocols," in *IEEE PIMRC*, (French Riviera, France), 2008.

[15] L. Lampe, R. Schober and S. Yiu, "Distributed space-time coding for multihop transmission in power line communication networks," *IEEE Journal of Selected Areas in Communications*, vol. 24, pp. 1389–1400, 2006.

[16] Y. Jing and B. Hassibi, "Distributed space-time trellis codes for a cooperative system," *IEEE Transactions on Wireless Communications*, vol. 5, pp. 3524–3536, 2006.

[17] J. Yuan, Z. Chen, Y. Li and L. Chu, "Distributed space-time trellis codes for a cooperative system," *IEEE Transactions on Wireless Communications*, vol. 8, pp. 4897–4905, 2009.

[18] L. Kong, R. G. Maunder, S. X. Ng and L. Hanzo, "Maximum-throughput irregular distributed space-time code for near-capacity cooperative communications," *IEEE Transactions on Vehicular Technology* , vol. 59, pp. 1511–1517, 2010.

[19] M. F. U. Butt, S. X. Ng and L. Hanzo, "Self-concatenated code design and its application in power-efficient cooperative communications," *IEEE Communications Surveys & Tutorials*, vol. 14, no. 3, pp. 858–883, 2012.

[20] M. Shirvanimoghaddam, Y. Li and B. Vucetic, "Distributed raptor coding for erasure channels: partially and fully coded cooperation," *IEEE Transactions on Communications*, vol. 61, pp. 3576–3589, 2013.

[21] Y. Li, M. S. Rahman, S. X. Ng and B. Vucetic, " Distributed soft coding with a soft input soft output (siso) relay encoder in parallel relay channels," *IEEE Transactions on Communications*, vol. 61, pp. 3660–3672, 2013.

[22] A. Bletsas, A. Khisti, D. P. Reed and A. Lippman, "A simple cooperative diversity method based on network path selection," *IEEE Journal on Selected Areas in Communications*, vol. 24, pp. 659–672, 2006.

[23] M. Ju and I. M. Kim, "Relay selection with anc and tdbc protocols in bidirectional relay networks," *IEEE Transactions on Communications*, vol. 58, pp. 3500–3511, 2010.

[24] C. Berrou, A. Glavieux and P. Thitimajshima, "Near Shannon limit error-correcting coding and decoding: Turbo-codes(1)," in *International Conference on Communications*, 1993.

[25] H. Mohammed and T. A. Khalaf, "Optimal positioning of relay node in wireless cooperative communication networks," in *Computer Engineering Conference (ICENCO), 2013 9th International*.

[26] H. Biao, L. Jie and S. Jinshu, "Optimal relay node placement for multi-pair cooperative communication in wireless networks," in *Wireless Communications and Networking Conference(WCNC)*, 2013.

[27] S. X. Ng, Y. Li, B. Vucetic and L. Hanzo, "Distributed irregular codes relying on decode-and-forward relays as code components," *IEEE Transactions on Vehicular Technology*, 2014.

[28] T. Cover and A. E. Gamal, "Capacity theorems for the relay channel," *IEEE Transactions on Information Theory*, vol. 25, pp. 572–584, 1979.

[29] J. G. Proakis, *Digital communications*. McGraw-Hill, New York, 2001.